

## Electrochemical impedance spectroscopy study of copper corrosion inhibition by PASP in 3% citric acid

Rui He<sup>a,b</sup>, Yuhua Gao<sup>a,b</sup>, Meifang Yan<sup>a,b,c</sup>, Lihui Zhang<sup>a,b</sup>, Zhenfa Liu<sup>a,b,\*</sup>

<sup>a</sup>*Institute of Energy Resources, Hebei Academy of sciences, Shijiazhuang, Hebei Province, China, emails: lzf63@sohu.com (Z.F. Liu), kxyherui@163.com (R. He), gaoyuhua77@163.com (Y.H. Gao), yanmeifang525@sina.com (M.F. Yan), zlhkxy@sohu.com (L.H. Zhang)*

<sup>b</sup>*Hebei Engineer Research Center for Water Saving in Industry, Shijiazhuang, Hebei Province, China*

<sup>c</sup>*Institute of Process Engineering, Chinese Academy of Sciences, State Key Laboratory of Multiphase Complex Systems, Beijing, China*

Received 21 February 2019; Accepted 1 July 2019

### ABSTRACT

The inhibitory action of polyaspartic acid (PASP) on copper in 3% citric acid was studied at a temperature range of 20°C–50°C using electrochemical impedance spectroscopy (EIS). The results revealed a good inhibitor efficiency of PASP within this concentration range. The inhibitor efficiency ( $\eta$ ) reached 91.5% with the PASP concentration of 1 g/L. Data obtained from EIS were analyzed to model the corrosion inhibition process through an equivalent circuit. The adsorption of PASP on the surface of copper was found to be consistent with the Langmuir adsorption isotherm.

**Keywords:** Copper; Polyaspartic acid (PASP); Citric acid; Corrosion inhibition; Electrochemical impedance spectroscopy (EIS)

### 1. Introduction

Copper is commonly used as a material in heating and cooling systems owing to its excellent thermal conductivity, good corrosion resistance and mechanical workability. Copper does not usually corrode in neutral media, but the atmosphere of industrial area often containing SO<sub>2</sub>, H<sub>2</sub>S, NO<sub>x</sub> and NO<sub>x</sub> results in the corrosion of the copper surface [1]. There are several ways of reducing the rate of corrosion in metals. Chemical inhibitors are one of the most practical means of protecting copper from corrosion in acidic media [2–4]. Polyaspartic acid (PASP) has been synthesized and used [5,6] as an environmentally friendly water treatment agent [7,8]. A new kind of polymer, PASP is biodegradable and the products of its degradation can be used as fertilizers. Therefore it is widely used in scale inhibition, cleaning and medicine [9–11]. Citric acid is an organic acid and has little causticity to metal.

### 2. Experimental

#### 2.1. Instruments and reagents

The experimental material was copper with an exposed area of 0.07 cm<sup>2</sup>. Copper electrode of the exposed surface was made by polishing mechanically to a smooth surface finish, using emery paper down to 1,200 grade, washing with distilled water and drying in the air. All of the solutions were prepared using distilled water. All of the electrochemical experiments were carried out in a three electrode set-up, using CHI660B (Shanghai, China) model electrochemical analyzer under computer control. The counter electrode was a platinum foil and saturated calomel electrode was used as the reference. All of the potential values refer to this electrode.

#### 2.2. Electrochemical techniques

Electrochemical measurements were carried out using a CHI660B electrochemical workstation (Chenhua Instruments, Inc., Shanghai, China). For potentiodynamic polarization experiments the voltage sweep range was from

\* Corresponding author.

–300 to +300 mV at a scan rate of 1 mV/s. Impedance spectra were recorded with an open corrosion potential in the frequency ranges from 0.05–100 kHz.

### 3. Results and discussion

#### 3.1. Potentiodynamic polarization

As shown in Fig. 1, the polarization behavior of copper in 3% citric acid at 20°C in the absence and presence of PASP was investigated. The electrochemical data are presented in Table 1. The inhibition efficiency ( $\eta$ ) at each concentration was calculated using the following equation [10]:

$$\eta = \frac{I_0 - I_{\text{corr}}}{I_0} \times 100\% \quad (1)$$

Here,  $I_0$  and  $I_{\text{corr}}$  are the corrosion densities in the absence and presence of the inhibitor, respectively. Upon the addition of different concentrations (0.00, 0.05, 0.10, 0.50, 1.00 and 2.00 g/L) of PASP, both the cathodic and anodic current densities were decreased. Based on the negative shift in the corrosion potential and the obvious decrease in the cathodic current density with the increasing PASP concentration, PASP is considered an inhibitor of the predominate cathodic effect to protect copper in citric acid [12,13]. From Fig. 1 and Table 1 we can see that PASP has a good inhibition effect on

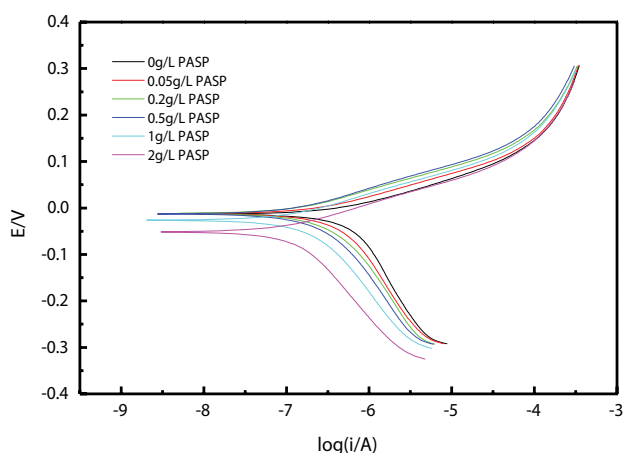


Fig. 1. Tafel plots of copper electrodes with different concentrations of PASP at 20°C.

Table 1

Electrochemical parameters of Tafel curves with different concentrations of PASP at 20°C

20°C	$E_{\text{corr}}$ (mV)	$b_a$ (mV)	$b_c$ (mV)	$i_{\text{corr}}$ (A)	$\eta$ (%)
0.00 g/L PASP	–0.034	8.321	3.538	$3.647 \times 10^{-6}$	~
0.05 g/L PASP	–0.028	9.331	3.249	$1.489 \times 10^{-6}$	53.7
0.10 g/L PASP	–0.026	10.00	3.961	$8.881 \times 10^{-7}$	75.6
0.50 g/L PASP	–0.033	10.34	4.207	$5.849 \times 10^{-7}$	84.0
1.00 g/L PASP	–0.044	11.89	4.419	$3.451 \times 10^{-7}$	90.5
2.00 g/L PASP	–0.051	15.15	5.038	$1.783 \times 10^{-7}$	95.1

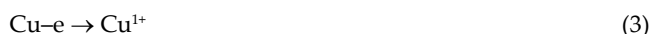
the corrosion of copper in citric acid and that the inhibition efficiency of PASP increases with increasing concentrations. In the experimental range, when PASP concentration was 1.00 g/L, the inhibition efficiency was 90.5% at 20°C.

#### 3.2. Electrochemical impedance spectroscopy (EIS) measurements

As shown in Fig. 2, electrochemical impedance analysis from 0.05 to 100 kHz at open circuit potential was also performed.

Fig. 2 shows the Nyquist plots for copper in the absence and presence of various concentrations of PASP at different temperature. The presence of inhibitor led to changes in the impedance plots in both shape and size. At higher frequencies, we can see a capacitive loop, which can be attributed to a faradaic process. Another loop involved the double-layer capacitance element [14]. In the copper corrosion in oxygenated solutions at  $E_{\text{corr}}$  the anodic reaction is copper dissolution and the cathodic reaction is oxygen reduction [15]. The reaction equation is as follows:

Anodic:



Cathodic:



As shown in the impedance diagrams, we can see that the size of the capacitive increases with the increasing concentration of PASP. This indicated that PASP increased the charge transfer resistance, and it had an inhibiting effect on copper corrosion. By considering the Nyquist spectra obtained at the temperature of below 40, we found that the Warburg impedance disappeared with the present PASP. At higher temperatures, the Warburg impedance appeared at different concentrations of PASP. The Nyquist plots changed, including both in the increase of capacitive loop and the disappearance of the Warburg impedance, indicating that increasing numbers of inhibitor molecules had adsorbed on the surface of by increasing the concentration of PASP, which showed that PASP had an inhibitory effect on copper corrosion [16]. The Warburg impedance could be attributed to oxygen transport from the bulk solution to the copper surface [17,18].

Fig. 3 shows a typical bode plots of the electrochemical impedance spectroscopy (EIS) spectra of the Cu electrode in

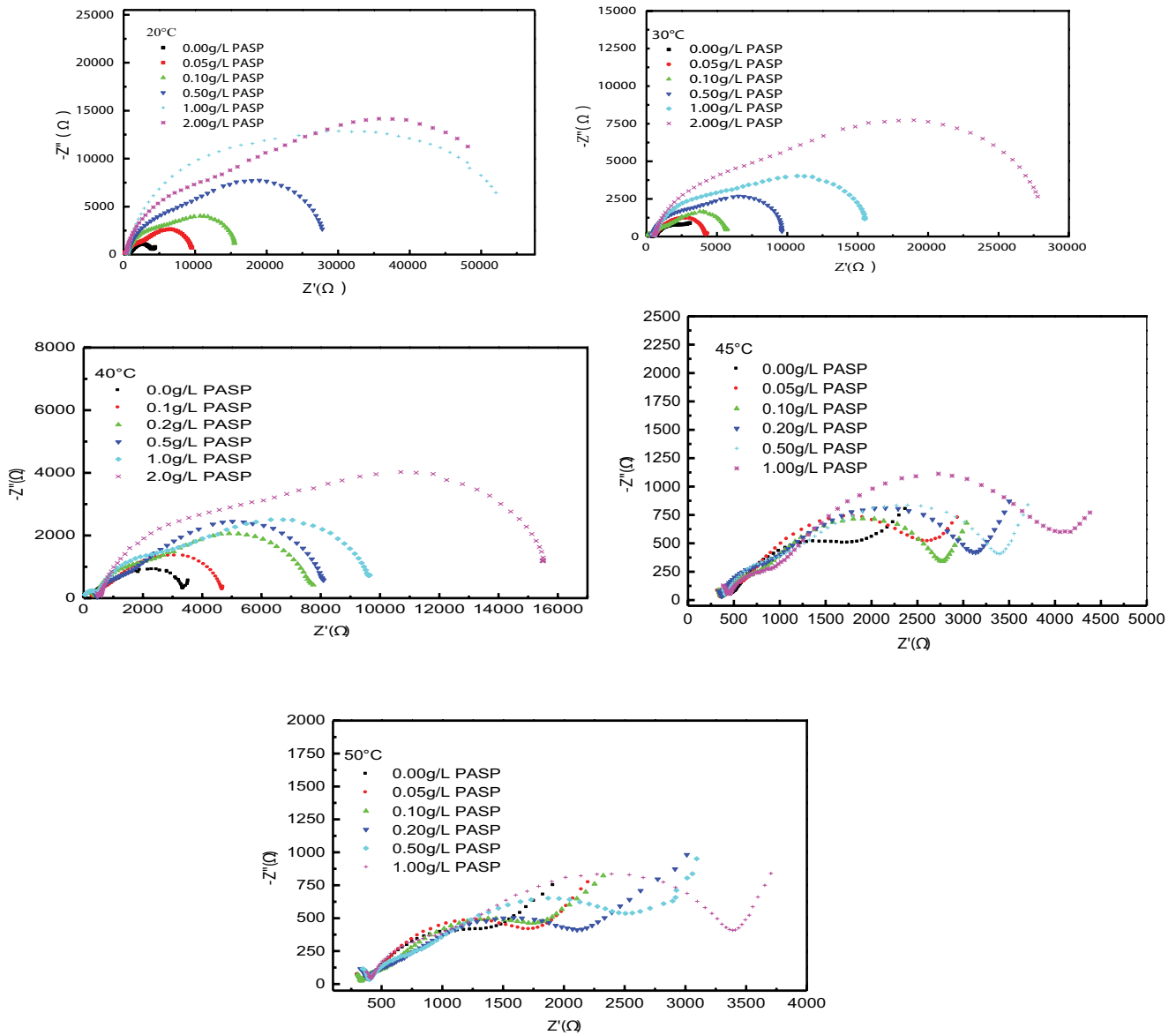


Fig. 2. Nyquist plots for purity copper in 3% Citric acid with different concentrations of PASP at different temperatures.

3% citric acid solution with different concentrations of PASP at 20°C. As shown in Fig. 3a, the impedance of copper in 3% citric acid showed slower values, which increased with the concentrations of PASP, especially at lower frequencies, which indicates the passivation of the surface against corrosion by adsorption of PASP molecules. We can see three peaks in Fig. 3b, which indicated that there are three time constants [19] in the corrosion process.

### 3.3. Equivalent circuit analysis

Using EQUIVCRT, an equivalent circuit was designed in order to fit the impedance spectra in Fig. 4 at 20°C, 30°C and 40°C, and Fig. 5 at 45°C and 50°C.

As shown in Figs. 4 and 5, three time constants are necessary to suitably reproduce impedance data. An equivalent circuit composed of three ladder parallel R-C circuit was used. In these circuits, R1 corresponds to the solution resistance. The high frequency circuit R-C corresponds to the capacitance and resistance of the surface film, most likely a compact oxide layer; the medium frequency circuit R-C corresponds to the double layer capacitance and charge transfer resistance. The lower frequency loop may be the resistance of adsorption and desorption process.

Figs. 6 and 7 show that the measured data and simulated data coincide very well. From Tables 2 and 3 we can also see that the X2 is less than 10<sup>-3</sup>, which indicated that the equivalent circuits are appropriate to the experimental system.

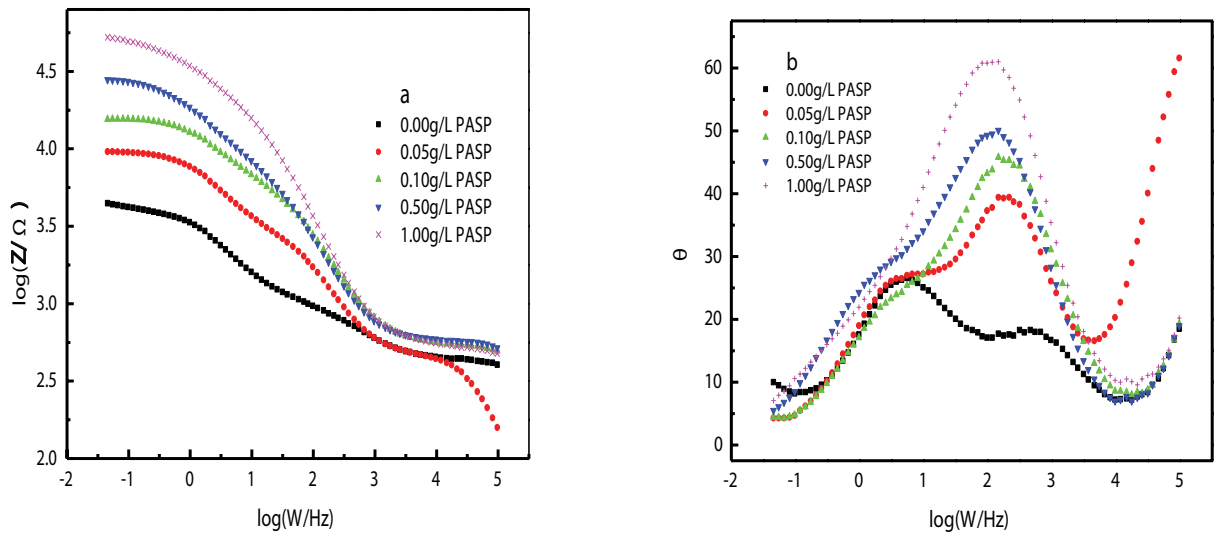


Fig. 3. Bode plots for purity copper electrode in 3% Citric acid solution with different concentrations of PASP at 20°C.

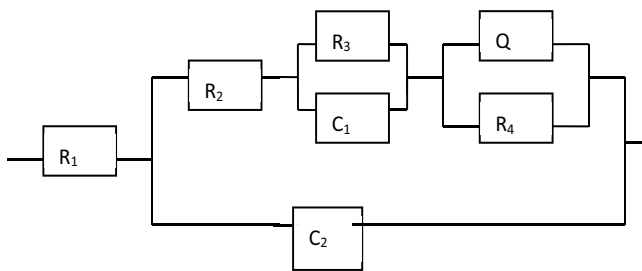


Fig. 4. Equivalent circuit of the Nyquist plots.

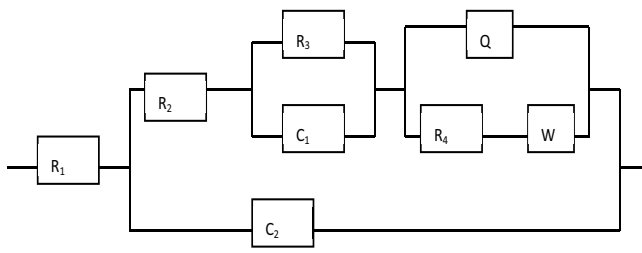


Fig. 5. Equivalent circuit of the Nyquist plots.

3.4. Adsorption isotherm

3.4.1. Isothermal adsorption research of PASP to copper at 20°C

To get a better understanding of the electrochemical process on the metal surface, adsorption characteristics at 20°C were also studied. The correlation coefficient was used to choose the isotherm that best fits the experimental data. The results showed that the adsorption behaviour of PASP followed Langmuir’s isotherm. Which can be expressed by the following relation [20]:

$$\frac{\theta}{(1-\theta)} = KC \tag{5}$$

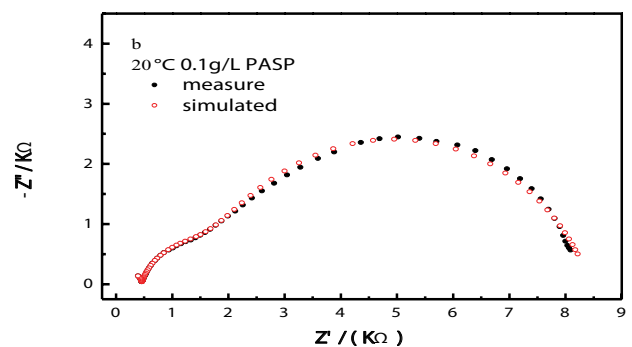
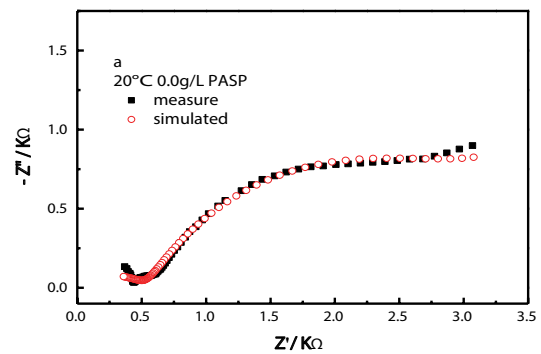


Fig. 6. Nyquist plots of comparing simulated results and measured results at 20°C.

Rearranging this equation gives:

$$\frac{C}{\theta} = \frac{1}{k} + C \tag{6}$$

Here  $\theta$  is the degree of surface coverage,  $C$  is the inhibitor concentration in the electrolyte, and  $K$  is the equilibrium constant for the process of adsorption. The plot of  $C/\theta$  against  $C$  gave a straight line as shown in Fig. 8. Therefore, the standard  $K$  can be calculated as  $K = 4.6 \times 10^4$  L/mol. The adsorption

constant of  $K$ , is related to the standard free energy of adsorption  $\Delta G^\circ$ , with the following equation:

$$K = \frac{\exp\left(\frac{-\Delta G^\circ}{RT}\right)}{55.5} \quad (7)$$

The value of 55.5 in the above equation is the concentration of water in solution in mol/L. The standard free energy of adsorption ( $\Delta G^\circ$ ) can be calculated,  $\Delta G^\circ = -36.14$  kJ/mol

### 3.4.2. Effects of temperature

The corrosion process can be considered to be an Arrhenius process [16], the inhibitor's apparent activation energy can be expressed as:

$$I_{\text{corr}} = A \exp\left(\frac{-E_a}{RT}\right) \quad (8)$$

where  $E_a$  is the activation energy, and  $A$  and  $R$  are the constants. Therefore, a plot of  $\ln I_{\text{corr}}$  against  $1/T$  will give a straight line from which  $E_a$  can be calculated based on its line

slope. The following equations without PASP (a) and with 0.5 g/L PASP (b) are as follows.

$$(a) \ln I_{\text{corr}} = \frac{-9.18953 - 0.97717}{T} \quad (9)$$

$$(b) \ln I_{\text{corr}} = \frac{-3.77452 - 2.99408}{T} \quad (10)$$

Fig. 9 shows the relationship about  $\ln I_{\text{corr}}$  against  $1/T$ , from which we can calculate the  $E_a = 30.31$  kJ/mol,  $E_a' = 64.62$  kJ/mol. It can be seen that  $E_a$  has a higher value in the presence of added PASP than that without it. It is obvious that this type of inhibition retarded the corrosion process at the experimental temperatures.

The Van't Hoff Eq. (21) is given as follows:

$$K = A \exp\left(\frac{-\Delta H^\circ}{RT}\right) \quad (11)$$

From Eqs. (6) and (11) the following equation is obtained:

$$\frac{\ln \theta}{(1-\theta)} = \frac{\ln A + \ln C - \Delta H^\circ}{RT} \quad (12)$$

The plot of  $\ln \theta/(1-\theta)$  against  $1/T$  in Fig. 10 will give a straight line from which we can calculate the  $\Delta H_m$  based on its line slope  $\Delta H = -60.148$  kJ/mol. According to the thermodynamic basic equation  $\Delta G = \Delta H - T\Delta S$ ,  $\Delta S$  can be calculated at the designed experimental temperatures,  $\Delta S = 156.3$  J/mol.

### 3.4.3. Thermodynamic parameters and discussion of PASP

The negative values of  $\Delta G$  ensure the spontaneity of the adsorption process and stability of the adsorbed layer on the copper surface. Generally, values of  $\Delta G$  around  $-20$  kJ/mol or lower are consistent with the electrostatic interaction between the charged molecules and the charged metal (physisorption), and these around  $-40$  kJ/mol or higher involve charge sharing or transfer from organic molecules to the metal surface to form a coordinate type of bond (chemisorption) [22–24].

The values of thermodynamic parameters for the adsorption of inhibitors can provide valuable information about the mechanism of corrosion inhibition.  $\Delta H < 0$  indicated that the adsorption process is an exothermic process. The  $\Delta S$  values in the presence of PASP are positive, meaning that an increase in disordering takes place in going from reactants to the metal-adsorbed species reaction complex.

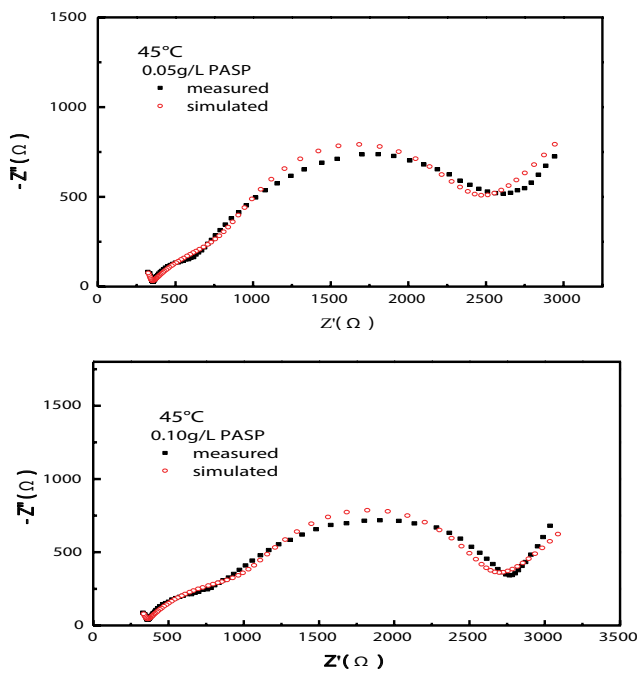


Fig. 7. Nyquist plots of comparing simulated results and measured results at 45°C.

Table 2  
Simulation results of Nyquist plot parameters at 20°C

Parameter concentration	$R_1/\Omega$	$R_2/\Omega$	$R_3/\Omega$	$C_1/F$	$Q$	$n$	$R_4/\Omega$	$C_2/F$	$X^2$	$\eta/\%$
0.0 g/L	12.4	295	359.2	$4 \times 10^{-6}$	$5 \times 10^{-4}$	0.69	2,507	$5 \times 10^{-9}$	$6 \times 10^{-4}$	~
0.1 g/L	14	320	585	$2 \times 10^{-6}$	$3 \times 10^{-4}$	0.67	7,836	$3 \times 10^{-9}$	$6 \times 10^{-4}$	68
0.5 g/L	26	486	1,132	$1.5 \times 10^{-6}$	$2 \times 10^{-4}$	0.61	9,977	$2 \times 10^{-9}$	$5 \times 10^{-4}$	75
1.0 g/L	36	513	2,031	$1.0 \times 10^{-6}$	$1 \times 10^{-5}$	0.60	15,341	$1 \times 10^{-9}$	$4 \times 10^{-4}$	84

Table 3  
Simulation results of Nyquist plot parameters at 45°C

Concentration	Parameter	Deviation	$X^2$	$\eta/\%$
0.00 g/L PASP	$R_1 = 2.16$	88.13	$6.42 \times 10^{-4}$	~
	$C_1 = 2.53 \times 10^{-4}$	15.01		
	$R_2 = 292$	5.09		
	$R_3 = 249$	8.51		
	$C_2 = 3.51 \times 10^{-8}$	13.3		
	$Q_1 = 4.47 \times 10^{-5}$	5.02		
	$n_1 = 0.666$	0.95		
	$R_4 = 726$	3.72		
	$W = 2.20 \times 10^{-3}$	3.04		
	$R_1 = 3.54$	89.2		
0.05 g/L PASP	$C_1 = 7.13 \times 10^{-5}$	5.50	$7.396 \times 10^{-4}$	44.2
	$R_2 = 335$	52.5		
	$R_3 = 732$	9.32		
	$C_2 = 1.00 \times 10^{-9}$	107		
	$Q_1 = 7.17 \times 10^{-5}$	19.8		
	$n_1 = 0.536$	5.05		
	$R_4 = 1198$	3.27		
	$W = 1.70 \times 10^{-3}$	5.26		
	$R_1 = 6.31$	28.5		
	$C_1 = 3.46 \times 10^{-5}$	5.10		
0.10 g/L PASP	$R_2 = 345$	51.3	$6.52 \times 10^{-4}$	49.9
	$R_3 = 898$	5.25		
	$C_2 = 9.48 \times 10^{-10}$	105		
	$Q_1 = 2.37 \times 10^{-5}$	15.2		
	$n_1 = 0.599$	3.32		
	$R_4 = 1271$	2.80		
	$W = 2.19 \times 10^{-3}$	5.85		
	$R_1 = 3.18$	36.3		
	$C_1 = 3.3 \times 10^{-5}$	3.44		
	$R_2 = 378$	20.5		
0.50 g/L PASP	$R_3 = 828$	3.41	$1.91 \times 10^{-4}$	60.1
	$C_2 = 1.07 \times 10^{-9}$	42.3		
	$Q_1 = 6.43 \times 10^{-6}$	8.88		
	$n_1 = 0.744$	1.57		
	$R_4 = 1967$	2.68		
	$W = 2.17 \times 10^{-3}$	4.78		

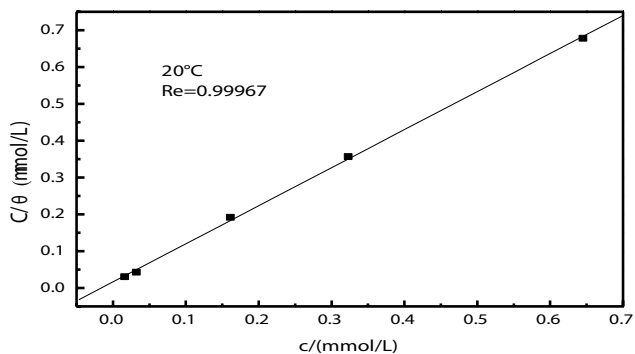


Fig. 8. Curve fitting of the corrosion data for copper electrode according to Langmuir thermodynamic kinetic model at 20°C.

#### 4. Conclusion

- The electrochemical measurements demonstrated that under these experimental conditions, the inhibition efficiency increased with increasing PASP concentration. The best performance efficiency of PASP on copper was 95.1%, which took place in 2.0 g/L PASP at 20°C. At the same concentration of PASP, the inhibition efficiency decreased with the temperature raised.
- Equivalent circuit was obtained using EQU software based on experimental data. At 20°C, 30°C and 40°C, the equivalent circuit is  $R(C[R(CR)(QR)])$ . At 45°C and 50°C the equivalent circuit is  $R(C[R(CR)(Q[RW])])$ .

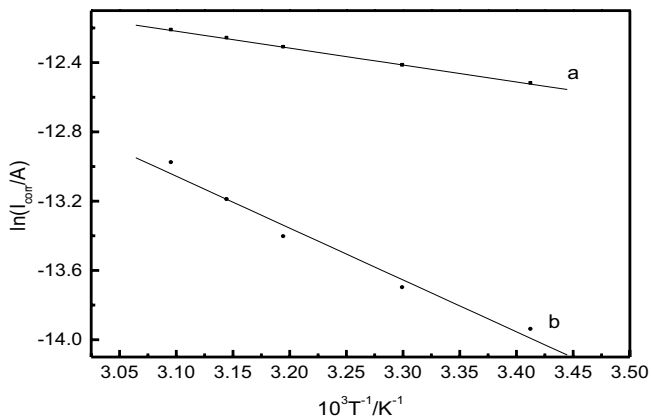


Fig. 9.  $I_{\text{corr}}$  vs.  $1/T$  curves of purity copper electrodes without (a) and with (b) 0.5 g/L PASP.

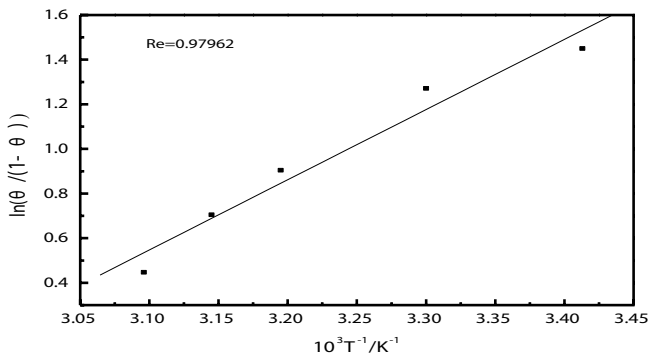


Fig. 10.  $\ln(\theta/(1-\theta)) \sim 1/T$  curves of copper electrodes with 0.5 g/L PASP.

- Under these experimental temperatures, the adsorption of PASP on copper surface was found to follow the Langmuir isotherm model, and it was a spontaneous exothermic process. This process may involve a mixture between physisorption and chemisorption.

### Acknowledgment

The work carried out was supported by the Fundamental Research Project of Hebei Province (18964005D), the Science and Technology Plan Project of Hebei Province (17393604D) and the National Natural Science Foundation of China (21376062), the Science and Technology Plan Project of Hebei Academy of Sciences (19705).

### References

- [1] M. Yan, Q. Tan, H. Li, L. Zhang, Z. Liu, Research on dynamic synergistic scale inhibition performance and mechanisms of ESA/IA/AMPS copolymer with electrostatic field, *Desal. Wat. Treat.*, 137 (2019) 34–40.
- [2] X. Li, G. Mu, Tween-40 as corrosion inhibitor for cold rolled steel in sulphuric acid: weight loss study, electrochemical characterization and AFM, *J. Appl. Surf. Sci.*, 252 (2005) 1254–1265.
- [3] M. Gao, H. Li, L. Zhang, X. Bai, Z. Liu, Study on synthesis scale inhibition performance and mechanism of ESA/IA/AMPS copolymer, *Fine Chem.*, 34 (2017) 42–47.
- [4] R. Cui, N. Gu, C. Li, Polyaspartic acid as a green corrosion inhibitor for carbon steel, *Mater. Corros.*, 60 (2009) 1–9.
- [5] R.J. Ross, K.C. Low, J.E. Shannon, Polyaspartate scale inhibitors—Biodegradable alternatives to polyacrylates, *Mater. Perform.*, 4 (1997) 36.
- [6] D.C. Silverman, D.J. Kalota, F.S. Stover, Effect of pH on corrosion inhibition of steel by polyaspartic acid, *Corrosion*, 11 (1995) 818–825.
- [7] M. Tomida, T. Nakato, S. Matsunami, T. Kakuchi, Convenient synthesis of high molecular weight poly (succinimide) by acid-catalysed polycondensation of L-aspartic acid, *Polymer*, 18 (1997) 4733–4736.
- [8] S.K. Wolk, G. Swift, Y.H. Paik, K.M. Yocom, R.L. Smith, E.S. Simon, One- and two-dimensional nuclear magnetic resonance characterization of poly (aspartic acid) prepared by thermal polymerization of L-aspartic acid, *Macromolecules*, 27 (1994) 7613–7620.
- [9] Y. Gao, L. Fan, L. Ward, Z. Liu, Synthesis of polyaspartic acid derivative and evaluation of its corrosion and scale inhibition performance in seawater utilization, *Desalination*, 365 (2015) 220–226.
- [10] S. Roweton, S.J. Huang, G. Swift, Poly (aspartic acid): synthesis, biodegradation, and current applications, *J. Environ. Polym. Degrad.*, 3 (1997) 175–181.
- [11] J.H. Todd, G.H. Hottendorf, Poly-L-aspartic acid protects cultured human proximal tubule cells against aminoglycoside-induced electrophysiological alterations, *Toxicol. Lett.*, 90 (1997) 217–221.
- [12] T. Vasudevan, B. Muralidharan, S. Muralidharan, S. Venkatakrishna Iyer, Inhibition of corrosion of mild steel in acidic solutions by quarternary salts of pyridinium bases, *Anti-Corros. Methods Mater.*, 2 (1998) 120–126.
- [13] E.E. Oguzie, Corrosion inhibition of mild steel in hydrochloric acid solution by methylene blue dye, *Mater. Lett.*, 59 (2005) 1076–1079.
- [14] O.E. Barcia, O.R. Mattos, Reaction model simulating the role of sulphate and chloride in anodic dissolution of iron, *Electrochim. Acta*, 10 (1990) 1601–1608.
- [15] W.H. Smyrl, *Electrochemistry and Corrosion on Homogeneous and Heterogeneous Metal Surfaces*, In: *Electrochemical Materials Science*, Springer, Boston, MA, 1981, pp. 97–149.
- [16] H.-L. Wang, H.-B. Fan, J.-S. Zheng, Corrosion inhibition of mild steel in hydrochloric acid solution by a mercapto-triazole compound, *Mater. Chem. Phys.*, 3 (2003) 655–661.
- [17] H. Ma, S. Chen, B. Yin, S. Zhao, X. Liu, Impedance spectroscopic study of corrosion inhibition of copper by surfactants in the acidic solutions, *Corros. Sci.*, 5 (2003) 867–882.
- [18] G. Quartarone, M. Battilana, L. Bonaldo, T. Tortato, Investigation of the inhibition effect of indole-3-carboxylic acid on the copper corrosion in 0.5 M H<sub>2</sub>SO<sub>4</sub>, *Corros. Sci.*, 50 (2008) 3467–3474.
- [19] H.O. Curkovic, E. Stupnisek-Lisac, H. Takenouti, Electrochemical quartz crystal microbalance and electrochemical impedance spectroscopy study of copper corrosion inhibition by imidazoles, *Corros. Sci.*, 10 (2009) 2342–2348.
- [20] R. Agrawal, T.K.G. Nambodhiri, The inhibition of sulphuric acid corrosion of 410 stainless steel by thioureas, *Corros. Sci.*, 1 (1990) 37–52.
- [21] D.D. Do, *Adsorption Analysis: Equilibria and Kinetics*, Vol. 2, Imperial College Press, London, 1998.
- [22] F.M. Donahue, K. Nobe, Theory of organic corrosion inhibitors adsorption and linear free energy relationships, *J. Electrochem. Soc.*, 9 (1965) 886–891.
- [23] E. Khamis, F. Bellucci, R.M. Latanision, E.S.H. El-Ashry, Acid corrosion inhibition of nickel by 2-(triphenylphosphoranylidene) succinic anhydride, *Corrosion*, 9 (1991) 677–686.
- [24] F. Bentiss, M. Lebrini, M. Lagrenée, Thermodynamic characterization of metal dissolution and inhibitor adsorption processes in mild steel/2, 5-bis (n-thienyl)-1, 3, 4-thiadiazoles/hydrochloric acid system, *Corros. Sci.*, 12 (2005) 2915–2931.